J Physiol 587.21 (2009) pp 5095–5106

The Journal of Physiology

Neurobeachin, a protein implicated in membrane protein traffic and autism, is required for the formation and functioning of central synapses

Lucian Medrihan[1], Astrid Rohlmann[2], Richard Fairless[2], Johanna Andrae[4], Markus Döring[4,5], Markus Missler[2], Weiqi Zhang[1,3] and Manfred W. Kilimann[4]

[1]*Center for Physiology, Georg-August University and DFG-Research Center of Molecular Physiology of the Brain, D-37073 Göttingen, Germany*
[2]*Institute of Anatomy and Molecular Neurobiology, University of Münster, D-48149 Münster, Germany*
[3]*Laboratory of Molecular Psychiatry, Department of Psychiatry, University of Münster, D-48149 Münster, Germany*
[4]*Department of Neuroscience, Uppsala University, S-75124 Uppsala, Sweden*
[5]*Department of Molecular Neurobiology, Max-Planck-Institute for Experimental Medicine, D-37075 Göttingen, Germany*

The development of neuronal networks in the brain requires the differentiation of functional synapses. Neurobeachin (Nbea) was identified as a putative regulator of membrane protein trafficking associated with tubulovesicular endomembranes and postsynaptic plasma membranes. Nbea is essential for evoked transmission at neuromuscular junctions, but its role in the central nervous system has not been characterized. Here, we have studied central synapses of a newly generated gene-trap knockout (KO) mouse line at embryonic day 18, because null-mutant mice are paralysed and die perinatally. Although the overall brain architecture was normal, we identified major abnormalities of synaptic function in mutant animals. In acute slices from the brainstem, both spontaneous excitatory and inhibitory postsynaptic currents were clearly reduced and failure rates of evoked inhibitory responses were markedly increased. In addition, the frequency of miniature excitatory and both the frequency and amplitudes of miniature inhibitory postsynaptic currents were severely diminished in KO mice, indicating a perturbation of both action potential-dependent and -independent transmitter release. Moreover, Nbea appears to be important for the formation and composition of central synapses because the area density of mature asymmetric contacts in the fetal brainstem was reduced to 30% of wild-type levels, and the expression levels of a subset of synaptic marker proteins were smaller than in littermate controls. Our data demonstrate for the first time a function of Nbea at central synapses that may be based on its presumed role in targeting membrane proteins to synaptic contacts, and are consistent with the 'excitatory–inhibitory imbalance' model of autism where Nbea gene rearrangements have been detected in some patients.

(Received 10 July 2009; accepted after revision 26 August 2009; first published online 1 September 2009)
Corresponding authors W. Zhang: Laboratory of Molecular Psychiatry, Department of Psychiatry, University of Münster, Albert-Schweitzer-Str. 11, 48149 Münster, Germany. Email: wzhang@uni-muenster.de and M. W. Kilimann: Department of Neuroscience, Uppsala University, Biomedical Center, Box 593, S-75124 Uppsala, Sweden. Email: manfred.kilimann@neuro.uu.se

Abbreviations EPPs, end-plate potentials; KO, knockout; mEPPs, miniature end-plate potentials; Nbea, neurobeachin; NH, hypoglossal nucleus; NMJ, neuromuscular junction; PSC, postsynaptic current; RVLM, rostral ventrolateral medulla; sEPSC, spontaneous excitatory postsynaptic current; sIPSC, spontaneous inhibitory postsynaptic current.

Introduction

The assembly of central nervous system synapses requires the polarized targeting of numerous proteins to pre- or postsynaptic compartments (Horton & Ehlers, 2003). With the exception of dense-core transport vesicles that carry 'active zone precursor' macromolecular aggregates (Zhai *et al.* 2001), the targeting mechanisms and trafficking pathways of synaptic components remain largely elusive. Neurobeachin (Nbea) is a member of the BEACH domain protein family whose members have been proposed to be involved in the subcellular

DOI: 10.1113/jphysiol.2009.178236

targeting of membrane proteins, and which are large (mostly 3000–4000 a.a.) cytosolic proteins that can peripherally associate with membranes. While yeast has only one BEACH domain protein, multicellular organisms such as *Dictyostelium*, plants, *C. elegans*, *Drosophila* and mammals contain about six BEACH domain proteins. This family shares a common domain architecture, in which the BEACH domain is preceded by an atypical PH domain and followed by a C-terminal WD40 repeat (De Lozanne, 2003). Although the structures of BEACH domains together with the interacting PH domains have been determined by X-ray crystallography, the function of the BEACH domain remains unknown (Jogl *et al.* 2002).

Nbea was discovered as a component of neuronal synapses, and found to be associated with polymorphic vesiculo-tubulo-cisternal endomembranes and postsynaptic plasma membranes. In particular, Nbea concentrates near the *trans*-Golgi network, and its membrane association is stimulated by GTP and antagonized by brefeldin A, reminiscent of vesicle-coat proteins and suggesting a functional link to the post-Golgi sorting or targeting of membrane proteins (Wang *et al.* 2000). Whereas Nbea expression seems to be restricted to neurons and endocrine cells, a ubiquitous isoform, Lrba, is up-regulated in stimulated immune cells and in cancer cells (Wang *et al.* 2001, 2004). Consistently, the single orthologues of Nbea and Lrba in *Drosophila* and *C. elegans*, Rugose and SEL-2, have been linked to the functioning and trafficking of growth factor receptors (EGFR, Notch; Shamloula *et al.* 2002; de Souza *et al.* 2007).

A functional role for Nbea in the peripheral nervous system was previously revealed in a null-mutant mouse line obtained by coincidental insertion mutagenesis (Su *et al.* 2004). Homozygous Nbea (−/−) mice were found to die immediately after birth apparently from breathing paralysis, and displayed a complete block of evoked transmission at the neuromuscular junction (NMJ) whereas nerve conduction, NMJ morphology and spontaneous quantal release were normal. However, important questions remained open from this study, most notably: are central synapses in the brain similarly dependent on Nbea? And if so, what aspect of neurotransmission and/or synapse structure is affected by Nbea?

Here, we examined synapses in the brainstem of Nbea-deficient mice that we derived from a gene-trap knockout (KO) mouse line. We observed that Nbea-deficient neurons display impaired spontaneous, miniature and evoked neurotransmission at excitatory and inhibitory synapses, but also reduced synapse numbers and perturbed composition of synaptic proteins, indicating a complex role for Nbea in the development and functioning of synapses and, consequently, of neuronal networks in the brain.

Methods

Generation of Nbea KO mice

Gene-modified mice were generated, maintained and biochemically analysed under approval of the Swedish Animal Welfare Agency. The gene-trap ES cell line RRK418 was obtained from BayGenomics, a member of the International Gene Trap Consortium. This Sv129-derived cell line has integrated the gene-trap vector pGT21xf in intron 6 of the Nbea gene. Genomic DNA from RRK418 around the integration site was amplified by PCR and sequenced. The vector was found to have inserted 385 bp downstream of exon 6. The first 389 bp of the gene-trap vector had been lost in the course of insertion, but the sequence loss was upstream of the vector's splice acceptor site and did not affect the function of the vector (Fig. 1*A*). ES cells were injected into C57Bl/6N blastocysts and implanted into foster mothers at the Uppsala University Transgenic Facility (UUTF). Chimeric male offspring were mated with C57Bl/6N females, and agouti pups were genotyped by PCR of genomic DNA. The line was maintained by backcrossing of heterozygous transgenic animals with C57Bl/6N mates. For PCR genotyping, three primers were employed in a single amplification reaction: a single forward primer for both the wild-type (WT) and the transgenic allele in exon 6 (Ex6F, 5′-TTTCGTACTAGCAAAGGAGTG-3′) and specific reverse primers for the WT and transgenic alleles in intron 6 (Int6/7R, 5′-GACTAAAAGATGGCAGCTCTC-3′) and in the gene-trap insert (Trap5′R, 5′-TTTGAGCACCAGAGGACATC-3′), respectively (Fig. 1*A* and *B*). Because of the length of the gene-trap insert (8.3 kb), the WT reverse primer produces an amplification product only from the unmodified allele. Immunoblots of 5% SDS-polyacrylamide gels (Fig. 1*B*) were probed with affinity-purified rabbit sera raised against isoform-specific sequences of mouse Nbea and Lrba ('region B'; Wang *et al.* 2000), and against the N-terminal region (a.a. 9–387) of mouse Rim1.

Electrophysiological recordings

All experiments were performed in accordance with the institutional regulations of animal welfare, were approved by the ethics committee of the University of Göttingen, and were in compliance with the policies and regulations outlined in Drummond (2009). Pregnant females (total number 25) were anaesthetized deeply by ether (in air) until no reflex response to noxious pinch of toe or tail was observed. Fetal mice (total number 75) were taken during anaesthesia. After removing the embryos, the females were decapitated during anaesthesia. The embryonic day 18 (E18) fetal littermate mice were decapitated and acute slices containing the rostral ventrolateral medulla (RVLM)

and hypoglossal nucleus (NH) were used for whole-cell recordings. The bath solution in all experiments consisted of (in mM): 118 NaCl, 3 KCl, 1.5 $CaCl_2$, 1 $MgCl_2$, 25 $NaHCO_3$, 1 NaH_2PO_4, 5 glucose, pH 7.4, aerated with 95% O_2 and 5% CO_2 and kept at 28–30°C. Evoked glutamatergic and GABAergic/glycinergic postsynaptic currents (PSCs) were recorded from hypoglossal neurons in the presence of 1 μM strychnine and 1 μM bicuculline or 10 μM 6-cyano-7-nitroquinoxaline-2,3-dione (CNQX), respectively. PSCs were evoked by 0.1 Hz field stimulations of axons of interneurons close to the RVLM using a bipolar platinum electrode. An isolation unit IsoFlex (A.M.P.I., Jerusalem, Israel) with a custom-built power supply was used to apply currents of supramaximal stimulation strength. The pipette solution for evoked glutamatergic and GABAergic/glycinergic PSC measurements contained (in mM): 140 potassium gluconate (glutamatergic PSCs) or 140 KCl (GABAergic/glycinergic PSCs), 1 $CaCl_2$, 10 EGTA, 2 $MgCl_2$, 4 Na_3ATP, 0.5 Na_3GTP, 10 Hepes, pH 7.3. Peak amplitudes were averaged from 25 consecutive responses. To monitor changes in input resistance, current responses to a −10 mV voltage step (20 ms) from a holding potential of −70 mV were recorded before every fifth stimulus. In all experiments the distance between the stimulation and recording electrodes was similar between slices of different genotypes. Spontaneous GABAergic/glycinergic and glutamatergic PSCs were recorded from neurons of the RVLM at a Cl^- reversal potential of about 0 mV in 10 μM CNQX or 1 μM strychnine and 1 μM bicuculline, respectively. Miniature GABAergic/glycinergic and glutamatergic PSCs (mIPSCs and mEPSCs) were recorded as described above, but in the presence of 0.5 μM tetrodotoxin (TTX). In all slices, spontaneous synaptic events were recorded for 5 min. The sample size for control slices was more than 200 events per slice, whereas the sample size for KO slices was 30–65 events per slice. Signals with amplitudes of at least 2 times above the background noise were selected, and the statistical significance was tested in each experiment. In all tested animals (control = 35, KO = 25), there were no significant differences in the noise levels between different genotypes. Voltage-activated currents were measured from neurons of the RVLM with patch electrodes containing (in mM): 110 CsCl, 30 TEA-Cl, (for Na^+ and Ca^{2+} current) or 140 KCl (for K^+ current), 1 $CaCl_2$, 10 EGTA, 2 $MgCl_2$, 4 Na_3ATP, 0.5 Na_3GTP, 10 Hepes pH 7.3, with 0.5 μM tetrodotoxin and 200 μM Cd^{2+} for blocking Na^+ and Ca^{2+}-current in the bath solution. After establishing the whole-cell configuration, membrane capacitance and membrane resistances were estimated from current transient induced by 20 mV hyperpolarization voltage commands from a holding potential of −70 mV. The serial resistance was compensated by 80%, and patches with a serial resistance of >20 MΩ, a membrane resistance of <0.8 GΩ, or leak currents of >150 pA were excluded. The membrane currents were filtered by a four-pole Bessel filter at a corner frequency of 2 kHz, and digitized at a sampling rate of 5 kHz using the DigiData 1200B interface (Axon Instruments/Molecular Devices, Sunnyvale, CA, USA). Currents were recorded and quantified as peak currents in response to voltage steps from −70 mV to 0 mV. The current measurements were corrected using the *P*/4 protocol that subtracts leak currents measured during four leak-subtraction prepulses applied immediately before each voltage step. Data acquisition and analysis were performed using commercially available software (pClamp 9.0 and AxoGraph 4.6 (Molecular Devices), and Prism 4 (GraphPad Software Inc., La Jolla, CA, USA)).

Biochemical analysis

E18 animals were obtained from timed-pregnant females under ether anaesthesia as described above. Brainstem samples from E18 WT and KO littermates were homogenized with a glass–Teflon homogenizer at setting 2000 rpm (10 strokes) in a buffer containing 1 mM EDTA, 20 mM Hepes pH 7.4, 0.1 mM PMSF, 2 μg ml^{-1} aprotinin, 2 μg ml^{-1} leupeptin. The homogenates were placed in ice-cold lysis buffer (1 : 1 Ripa with 1% NP-40), incubated at 4°C for 2 h, and centrifuged in a microliter centrifuge at 14 000 rpm at 4°C for 30 min. The protein concentration of supernatants was determined by a Lowry assay using the total protein kit from Sigma with bovine serum albumin (Sigma-Aldrich, St Louis, MO, USA) as a standard. Thirty micrograms of sample was resuspended in 3× loading buffer (62.5 mM Tris-HCl, 20% glycerol, 6% SDS, 0.01% bromphenol blue, 10% β-mercaptoethanol), boiled at 100°C for 5 min, and separated by 10% SDS-PAGE. Proteins were transferred to Hybond nitrocellulose membrane (GE Healthcare, Little Chalfont, UK) and probed with antibodies against the following: $GABA_AR$ α1 and GlycineR $\alpha 1 + \alpha 2$ (Abcam, Cambridge, UK); VIAAT, VGluT1/2 (Chemicon/Millipore, Temecula, CA, USA); PSD-95 (Antibodies Inc., Davis, CA, USA); synaptophysin, synaptobrevin, synaptotagmin, synapsin I, Rab3A, syntaxin 1, SV2, SNAP-25, gephyrin, Munc-18, synaptoporin, dynamin, complexin II (Synaptic Systems, Göttingen, Germany); Hsp70 (Santa Cruz Biotechnology, Santa Cruz, CA, USA). Proteins were detected by AceGlow chemiluminescence detection reagents and imaging system Chemi-Smart 5000 (Peqlab GmbH, Erlangen, Germany). The quantitative analysis of immunoblots was done using Bio-1D software (Vilbert-Lourmat, Torcy, France), and included the results from tissue samples of at least three WT–KO littermate mouse pairs.

Electron microscopy

E18 animals were obtained from timed-pregnant females, and 400 μm coronal brainstem sections were

cut as for electrophysiological experiments. Vibratome sections were immersion-fixed with freshly prepared 0.5% paraformaldehyde and 2% glutaraldehyde in 0.1 M cacodylate buffer overnight. Osmicated sections containing the RVLM and NH were flat-embedded in epoxy resin following standard techniques, and ultramicrotome sections with uranyl actetate/lead citrate contrast were analysed on a transmission electron microscope (Phillips CM10) essentially as described (Missler *et al.* 2003; Varoqueaux *et al.* 2006). Statistical analysis was performed with Student's *t* test (GraphPad Prism software).

Data analysis

All data are presented as means ± S.E.M. Numbers on the bars in the bar graphs indicate the number of neurons/mice tested for each genotype. It is important to note that, although slices of E18 were recorded, none of the recorded neurons was silent. Only KO cells with more than 30 events (sE/IPSCs or mE/IPSCs) and WT cells with more that 200 events were selected for statistical evaluation, to avoid a bias towards small sample sizes. Significance was tested by Student's two-tailed *t* test with or without Welch's correction.

Results

Neurobeachin deficiency impairs neurotransmission at excitatory and inhibitory central synapses

We generated Nbea KO mice from the gene-trap cell line RRK418. The gene-trap vector had inserted into intron 6 of the Nbea gene, after 314 a.a. (10%) of the coding sequence (Fig. 1*A*; Methods). RT-PCR of brain RNA from homozygous KO animals indicated efficient abortive splicing from exon 6 onto the gene-trap splice acceptor (see legend to Fig. 1*A*), and Western blot analysis of brain homogenates gave no or at most a very faint Nbea protein signal even after long exposure times (Fig. 1*B*; maximally 2% of wild-type expression by densitometry). There was no compensatory up-regulation of Lrba, the ubiquitous isoform of Nbea (Fig. 1*B*). Newborn homozygous mutant pups were cyanotic, displayed no spontaneous movement or reactions to tactile stimuli, usually had an umbilical hernia, and died within minutes after birth. These findings are consistent with the perinatally lethal phenotype of an earlier Nbea-deficient mouse line created by random antisense insertion of several copies of a promoterless growth hormone minigene into intron 1 of the Nbea gene (Su *et al.* 2004). We also observed the hump (Fig. 1*C*) that Su *et al.* (2004) have characterized as an enlarged interscapular fat pad. We excluded possible non-neuronal reasons for the primary asphyxia in Nbea KO mice by analysing the gross anatomy of most vital organs such as heart or lung that showed no obvious abnormality that might explain the lethal phenotype (data not shown).

We have previously used the brainstem as a model system to study synaptic function in perinatally lethal mutant mice, combining electrophysiological, biochemical and ultrastructural approaches (Missler *et al.* 2003; Zhang *et al.* 2005; Varoqueaux *et al.* 2006). At early stages, the synapses and networks in the brainstem are more mature than, for example, in neocortex or hippocampus, allowing the use of acute slices to study the role of Nbea in the central nervous system. In particular, the slice preparation contains the respiratory network that is fully functional at embryonic day 18, including the network between the rostral ventrolateral medulla (RVLM) and the hypoglossal nucleus (NH; Smith *et al.* 1991).

To exclude the possibility that Nbea deficiency causes a general impairment of neuronal excitability, we first tested the membrane properties and the integrity of ion channels in RVLM neurons of KO mice by measuring whole-cell currents of Na^+, K^+ and Ca^{2+} channels (Fig. 1*D–F*). Whole-cell recordings of voltage-activated Na^+ currents were similar between control and KO mice (control: 91.3 ± 12.5 pA pF^{-1}; KO: 79.3 ± 8.6 pA pF^{-1}; not significant (n.s.), Fig. 1*D*). Similarly, no significant changes could be seen in current density of either voltage-activated K^+ channels (control: 134.6 ± 14.4 pA pF^{-1}; KO: 151.3 ± 18.6 pA pF^{-1}; n.s., Fig. 1*E*) or Ca^{2+} channels (control: 14.6 ± 2.8 pA pF^{-1}; KO: 15.6 ± 1.7 pA pF^{-1}; n.s., Fig. 1*F*). Likewise, no differences could be found in input resistance or membrane capacitance between neurons of KO and control mice (data not shown). Although these whole-cell recordings do not exclude an impairment of minor subsets of ion channels, e.g. at synapses, these results indicate that deletion of Nbea did not change the overall excitability or the membrane properties of RVLM neurons. In contrast, when we monitored spontaneous excitatory postsynaptic currents (sEPSCs) using whole-cell recording from NH neurons in the presence of 1 μM bicuculline and 1 μM strychnine, we observed strongly impaired synaptic transmission. The frequency of sEPSCs in hypoglossal neurons was decreased by 40% in Nbea knockout mice (Fig. 2*A* and *C*; control: 2.5 ± 0.3 Hz; KO: 1.6 ± 0.2 Hz; $P < 0.01$), while the amplitude was not affected (Fig. 2*A*,*B*; control: 22.8 ± 0.6 pA; KO: 23.8 ± 0.5 pA; n.s.), indicating a lower network activity in KO animals. To distinguish if this reduction is entirely due to less action potential-driven release or also affects AP-independent events, we next measured so-called 'mini events'. The frequency of miniature EPSCs in the presence of 0.5 μM TTX was also markedly reduced in Nbea-KO mice (Fig. 2*D*, *F* and *H*; control: 1.1 ± 0.1; KO: 0.2 ± 0.05; $P < 0.001$), whereas the amplitude of mEPSCs (Fig. 2*D*, *E* and *G*; control: 24.7 ± 0.6 pA; KO: 23.7 ± 1.3 pA; n.s.) and the rise- and

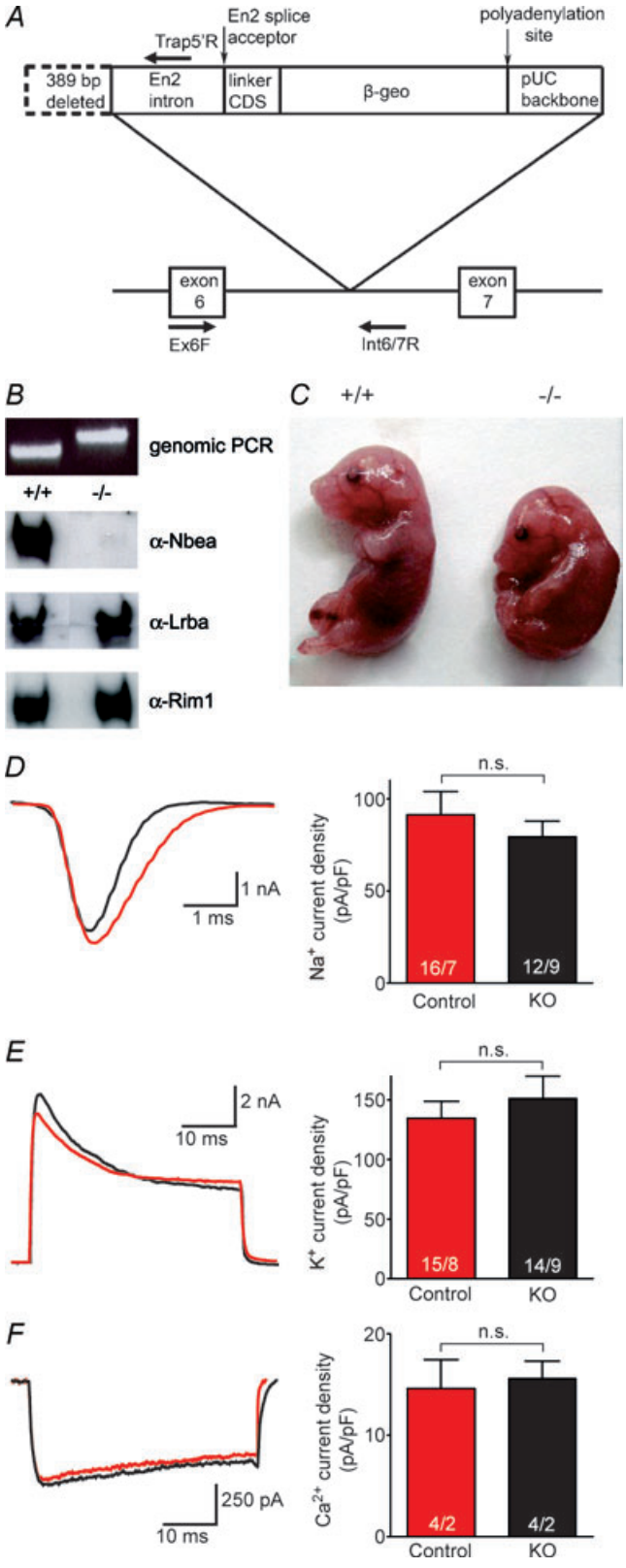

Figure 1. Neurobeachin null-mutant mice created by gene-trap
A, insertion of the gene-trap vector pGT21xf in intron 6 of the Nbea gene. RT-PCR of brain RNA from embryonic day 18 (E18) or postnatal day 1 (P1) homozygous Nbea KO mice produced amplification products between exon1 and exon 3 and between exon 6 and gene-trap sequences, but not between exon 7 and exon 9 sequences in contrast to RNA from wild-type animals (data not shown), indicating efficient abortive splicing from exon 6 onto the gene-trap splice acceptor. The Nbea gene has a total of 57 exons. *B*, PCR genotyping of wild-type and KO mice employing the primers shown in *A* (upper panel), and immunoblots demonstrating virtually complete loss of Nbea protein in KO mouse brain whereas expression of Lrba and (as control) Rim1 are unaffected (lower panels). *C*, typical atonic posture and interscapular hump of a gene-trap Nbea-KO mouse (right) at E18 delivered by caesarean section, compared to a WT littermate (left). *D–F*, representative traces of voltage-activated Na^+ (*D*), K^+ (*E*) and Ca^{2+} (*F*) currents and the corresponding mean current densities from WT (red) and neurobeachin KO (black) neurons demonstrate unaffected general neuronal excitability. Data shown are means ± S.E.M. The numbers on the bars represent the number of neurons/mice tested.

decay-times of mEPSCs ($P = 0.09$; Table 1) were not significantly changed between the genotypes, suggesting that the release machinery of excitatory terminals is impaired in the absence of Nbea. However, while we observed a strong reduction in synaptic transmission, we never recorded a 'silent' neuron with no activity at all in Nbea KO mice, suggesting a generalized impairment of synaptic efficacy (e.g. through a delay in synaptic maturation) rather than a complete dysfunction of a subpopulation of neurons.

To test this interpretation and to evaluate if inhibitory synapses were also affected by the Nbea deletion, we monitored spontaneous glycine- and GABAergic inhibitory postsynaptic currents (sIPSCs) in RVLM neurons in the presence of 10 μM CNQX and 40 μM 2-amino-5-phosphonovaleric acid (APV). Both the amplitude (Fig. 3*A* and *B*; control: 93.7 ± 5.8 pA; KO: 33.7 ± 6.7 pA; $P < 0.001$) and the frequency (Fig. 3*A* and *C*; control: 2.1 ± 0.2 Hz; KO: 0.35 ± 0.1 Hz; $P < 0.001$) of sIPSCs were strongly reduced in Nbea KO mice. This reduction in spontaneous IPSCs is even more pronounced than the impairment of excitatory transmission (Fig. 2). Analysis of miniature inhibitory postsynaptic currents (mIPSCs) revealed a similarly dramatic reduction of the frequency of mIPSCs in Nbea KO mice (Fig. 3*D*, *F* and *H*; control: 0.7 ± 0.2 Hz; KO: 0.05 ± 0.04 Hz; $P < 0.001$). The averaged amplitudes of the remaining miniature events in KO neurons were only moderately decreased compared to littermate controls (Fig. 3*D*, *E* and *G*; control: 44.4 ± 4.2 pA; KO: 25.3 ± 4.9 pA; $P < 0.01$), and the rise- and decay-times of mIPSCs were not significantly different between the KO and control mice (Table 1). As noted for excitatory activity (above), we observed a general reduction but not a complete absence of IPSCs in all KO neurons tested. Interestingly, the average amplitude of mIPSCs in KO neurons was only 25% smaller than the amplitude of sIPSCs, indicating that in absence of Nbea, spontaneous network activity did not contain many multivesicular, AP-driven IPSCs. This may indicate

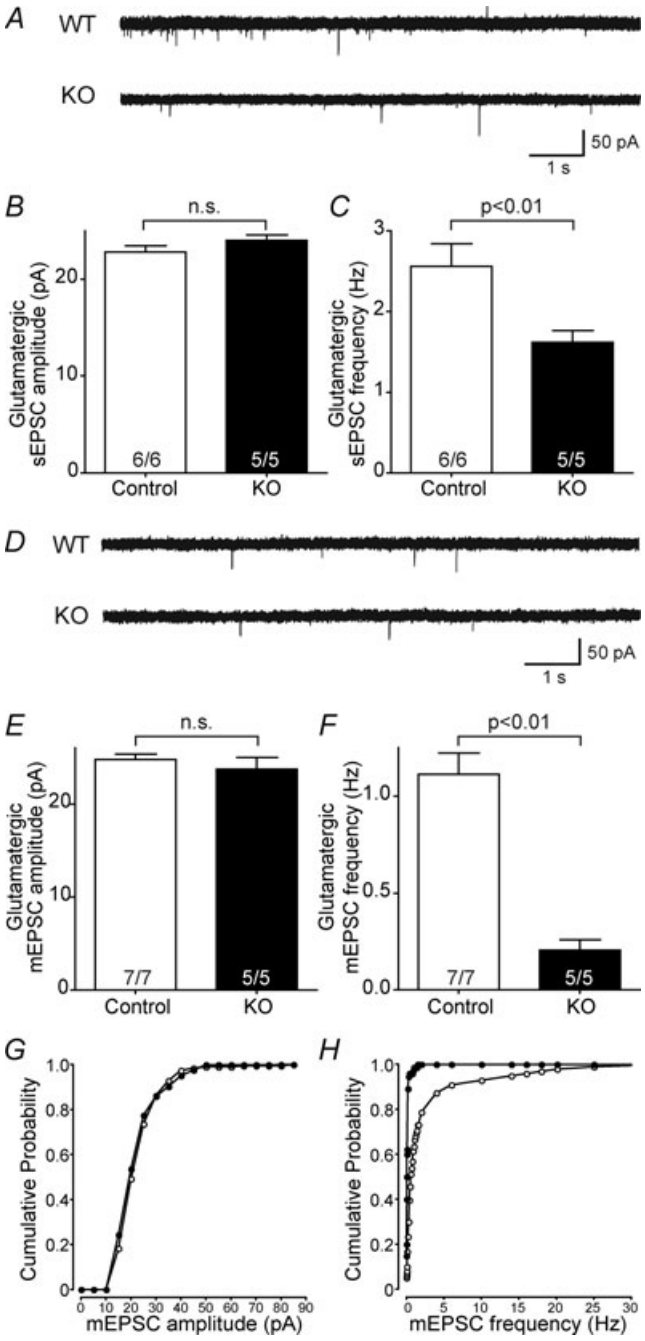

Figure 2. Glutamatergic neurotransmission is impaired in neurobeachin KO mice

A, representative recordings of pharmacologically isolated glutamatergic spontaneous sEPSCs in brainstem RVLM neurons. *B* and *C*, averaged amplitude (*B*) and frequency (*C*) of glutamatergic spontaneous sEPSCs in WT and mutant neurons. *D*, representative recordings of pharmacologically isolated glutamatergic miniature mEPSCs in brainstem RVLM neurons. *E* and *F*, averaged amplitude (*E*) and frequency (*F*) of glutamatergic miniature mEPSCs in WT and mutant neurons. *G* and *H*, cumulative distribution of the amplitude and frequency of glutamatergic mEPSCs in RVLM neurons of littermate control (open circles) and neurobeachin KO mice (filled circles). Data shown are means ± S.E.M. The numbers on the bars represent the number of neurons/mice tested.

Table 1. Kinetics of miniature PSCs in wild-type and Nbea KO mice

	Rise time (10–90%) (ms)	Decay time (ms)	Half-width (ms)	Area (pA. ms)
mIPSC				
WT	2.0 ± 0.6	46.2 ± 13.0	11.5 ± 0.9	716 ± 167
KO	2.2 ± 0.5	29.9 ± 13.5	10.0 ± 1.8	652 ± 266
mEPSC				
WT	1.7 ± 0.4	32.5 ± 18.0	5.9 ± 1.0	294 ± 50
KO	1.6 ± 0.5	23.8 ± 9.5	3.4 ± 0.4	172 ± 27

All data represent means ± S.E.M. Decay was fitted with a double exponential equation as described in Methods.

that the central nervous system of Nbea-deficient mice is more immature than in wild-type littermates.

Changes in frequency of spontaneous or miniature postsynaptic currents are the most prominent finding in our physiological analysis of both excitatory and inhibitory central synapses in Nbea null-mutant mice. However, while amplitudes were reduced in IPSCs, no significant changes of spontaneous or mini amplitudes were observed in EPSCs. To further explore the reduced inhibitory amplitudes, we evoked IPSCs of NH neurons in the presence of 10 μM CNQX and 40 μM APV by extracellular field stimulation in the RVLM region. In contrast to spontaneous or mini responses, the averaged amplitude of eIPSCs did not differ significantly between control and Nbea KO mice (Fig. 4*A* and *B*; control: 118.7 ± 54.8 pA; KO: 93.7 ± 55.3 pA; n.s.). However, the failure rate of stimulation-evoked IPSCs was dramatically elevated 22-fold from 3 ± 1.9% in control mice to 66.4 ± 11.8% in KO mice at the same stimulation strength ($P < 0.001$; Fig. 4*A* and *C*), indicating a massive impairment of excitation–release coupling but, once postsynaptic responses were elicited by synchronized extracellular stimulations, the evoked IPSCs were similar in amplitude.

Neurobeachin may be required for synapse maturation in the central nervous system

Since the electrophysiological findings shown above may be caused by various cellular defects, e.g. pre- and/or post-synaptic impairments, changes in synapse and/or vesicle numbers, etc., we started to explore which molecular components of synapses are affected in Nbea KO mice (Fig. 5). Expression levels of numerous pre- and post-synaptic marker proteins were analysed and quantified by immunoblotting (Fig. 5*A* and *B*). While the levels of most proteins tested were unchanged in brainstem lysates of mutant animals, the relative amounts of the synaptic vesicle (SV) membrane proteins synaptophysin and SV2, as well as of the SV-associated adaptor/scaffolding proteins synapsin I and Mint-1 were significantly reduced by

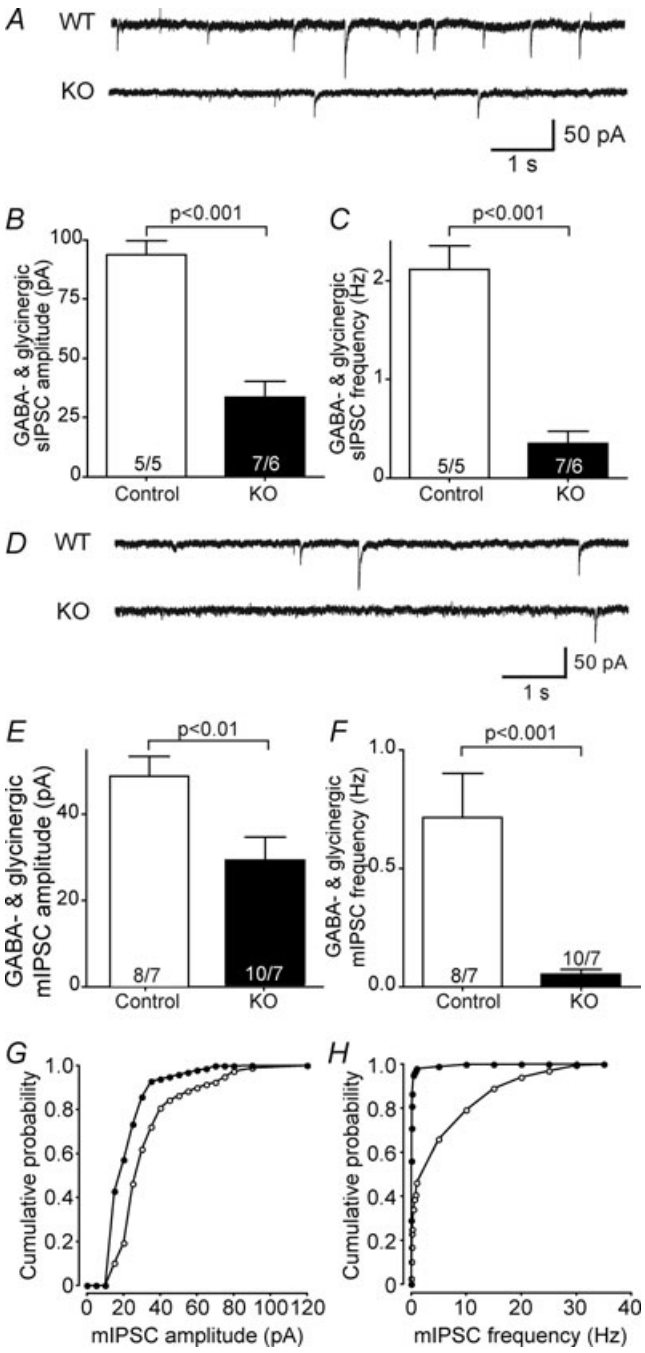

Figure 3. Inhibitory synaptic transmission is largely abolished in neurobeachin KO mice

A, representative recordings of pharmacologically isolated glycinergic and GABAergic spontaneous sIPSCs in brainstem RVLM neurons. *B* and *C*, averaged amplitude (*B*) and frequency (*C*) of glycinergic and GABAergic spontaneous sIPSCs in WT and mutant neurons. *D*, representative recordings of glycinergic and GABAergic miniature mIPSCs in brainstem RVLM neurons. *E* and *F*, averaged amplitude (*E*) and frequency (*F*) of glycinergic and GABAergic miniature mIPSCs in WT and mutant neurons. *G* and *H*, cumulative distribution of the amplitude and frequency of glycinergic and GABAergic mIPSCs in RVLM neurons of littermate control (open circles) and neurobeachin KO mice (filled circles). Data shown are means ± S.E.M. The numbers on the bars represent the number of neurons/mice tested.

25–40% (Fig. 5*B*). In contrast, other SV membrane proteins such as synaptotagmin or synaptoporin and other active zone molecules such as Munc18 or Rab3A were not changed in KO animals, indicating that Nbea specifically affects the overall levels of a subset of synaptic proteins. The selective reduction of a subset of intrinsic and peripheral SV proteins is also remarkable because in many other KO models with strongly affected neurotransmission, synaptic protein levels were not changed (e.g. Verhage *et al.* 2000; Missler *et al.* 2003; Varoqueaux *et al.* 2006). Our biochemical results do not exclude the possibility that additional proteins, e.g. postsynaptic receptors, are affected by the deletion of Nbea in alternative ways (altering protein targeting but not overall abundance), e.g. by altering the ratio between the synaptic/extrasynaptic populations or the amount in soluble/insoluble fraction which were not tested for in our assay.

Although the morphology of neuromuscular junctions was found to be normal in an earlier study of Nbea-deficient mice (Su *et al.* 2004), our observation of specifically reduced, mostly presynaptic, protein levels in KO mice raised the possibility that deletion of Nbea may have an effect, for example, on the number of synaptic terminals or vesicles in the central nervous system. To investigate brainstem synapses ultrastructurally, we performed electron microscopy predominantly in the rostral ventrolateral medulla (RVLM) of E18 Nbea-deficient and littermate control mice (Fig. 6). The area density, i.e. the number of synaptic contacts per square micrometre, was determined

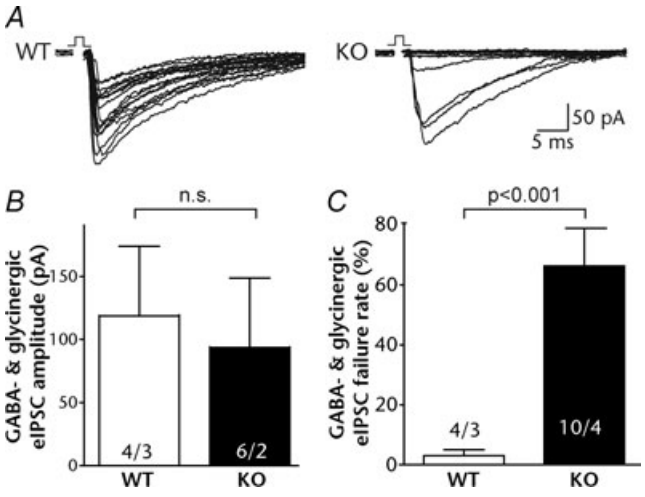

Figure 4. Neurobeachin KO mice display an increased failure rate

A–C, sample traces (*A*), averaged amplitudes (*B*), and failure rates (*C*) of glycinergic and GABAergic evoked eIPSC in WT and mutant neurons in response to extracellular stimulation. Data shown are means ± S.E.M. The numbers on the bars represent the number of neurons/mice tested.

on ultrathin sections of embedded coronal brainstem slices including the RVLM, like those used for electrophysiological recordings. Our analysis revealed that normal asymmetric or type 1 synapses (Fig. 6*A* and *B*) could be observed in KO mice, but their area density was reduced to about 30% of controls (control: 33.7 ± 5.25 per 10 000 μm^2; KO: 10.3 ± 3.18 per 10 000 μm^2; $n = 3$ for each genotype; $P = 0.01$), consistent with the strongly reduced mini EPSC frequency in the patch-clamp measurements (Fig. 2*F*). In addition, mutant presynaptic terminals appeared to contain fewer vesicles (Fig. 6*B*), but SV numbers varied too widely to allow statistically meaningful quantification in the material available for this study (data not shown). In contrast to type 1 terminals, no large difference in area density was found for symmetric or type 2 synaptic contacts (control: 20.3 ± 2.19 per 10 000 μm^2; KO: 16.3 ± 3.18 per 10 000 μm^2; $n = 3$ for each genotype; n.s.), although the reduction in mIPSC frequency (Fig. 3*C*) was even greater than for mEPSCs. However, so-called 'intermediate junctions' (immature type 1 contacts) that are especially abundant during development (Missler *et al.* 1993) may obscure the actual number of type 2 synapses, which they resemble. Therefore, a reduction also of inhibitory synapses remains possible. Comparing the morphology of type 2-like contacts in control and Nbea KO brainstems (Fig. 6*C* and *D*), many of the mutant synapses indeed appeared somewhat uncharacteristic with respect to SV distribution, cleft morphology and inapparent postsynaptic density (Fig. 6*D*, and data not shown), suggesting that a proportion of them may in fact be immature type 1 contacts. The reduced synapse density may contribute to the reduced frequencies of miniature and action potential-driven spontaneous PSCs observed in the electrophysiological recordings.

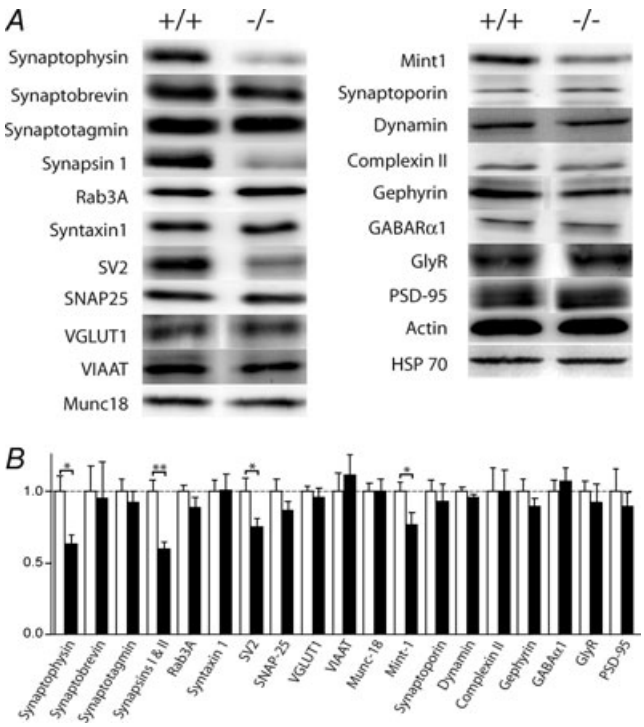

Figure 5. Expression levels of a subset of synaptic proteins are decreased in neurobeachin KO mice
A, representative immunoblots of synaptic proteins in littermate WT and Nbea KO mice, using actin and heat-shock protein 70 (Hsp70) as input control. *B*, quantitative analysis of the protein levels from brainstem lysates of littermate wild-type (open bars, WT) and Nbea-deficient mice (filled bars, KO) at embryonic day E18. Data are shown as means ± S.E.M. Three pairs of littermate WT and KO mice were used for each analysis.

Discussion

Our data demonstrate that the BEACH domain protein, Nbea, is essential for the function of central synapses. Deletion of Nbea in mice causes (i) reduced miniature and action potential-driven transmission at excitatory and inhibitory synapses (Figs 2–4); (ii) modifications in the composition of synaptic proteins (Fig. 5); (iii) a reduced number of synaptic contacts (Fig. 6) - in the absence of global changes of cellular excitability (Fig. 1) and major alterations of brain architecture.

The cellular functions and molecular mechanisms of any BEACH proteins are still poorly understood, but evidence is accumulating for roles in membrane dynamics, and particularly in the subcellular trafficking of membrane proteins. For example, mutations of LYST, occurring in human Chediak–Higashi syndrome and the *beige* mouse, perturb the biogenesis of lysosomes and lysosome-derived secretory vesicles, leading to defects in immune defence, pigmentation, thrombocyte function and nervous system function. This LYST deficiency phenotype seems to be caused by the mistargeting of multiple membrane proteins between the *trans*-Golgi network, endosomes, lysosomes and the plasma membrane (Faigle *et al.* 1998). Along this line, the single *C. elegans* orthologue of mammalian Nbea and Lrba, SEL-2, was shown to be a negative regulator of lin-12/Notch activity, and to affect the endosomal trafficking of LET-23/EGFR in polarized epithelial cells (de Souza *et al.* 2007). *Dictyostelium* LvsA is essential for cytokinesis and contractile vacuole function (De Lozanne, 2003). Mammalian Alfy is implicated in autophagy, whereas deficiency of its *Drosophila* orthologue, blue cheese, causes a complex neurodegenerative phenotype with ubiquitinated protein aggregates that include amyloid precursor-like protein, and perturbations of Rab11 function, axonal transport and synaptic morphogenesis (Finley *et al.* 2003; Simonsen *et al.* 2004; Khodosh *et al.* 2006; Lim & Kraut, 2009). Finally, the only yeast BEACH protein, bph1, is involved in vacuolar protein sorting (Shiflett *et al.* 2004). The bph1 phenotype

is mild, suggesting that the diversity and biological importance of BEACH proteins grew with the increasing complexity of membrane architecture, membrane polarity and membrane protein traffic pathways in multicellular organisms, and particularly in the nervous system.

Our findings indicate a putative impact of Nbea deletion on several aspects of synapses (stimulus–release coupling, vesicle fusion, postsynaptic signal amplitude, formation or maturation of synaptic contacts), consistent with the working hypothesis that Nbea is important for the targeting of multiple neuronal membrane proteins. The observation that the expression levels of a few synaptic proteins are selectively reduced in the Nbea KO mice supports this notion. The affected proteins belong to different molecular and functional categories (vesicle membrane proteins, adaptor/scaffolding proteins), and they may be directly or indirectly affected by Nbea. The protein levels determined by immunoblotting represent an average of the changes in multiple types of neurons and synapses at various stages of development, and the reduced overall amounts may result from decreased expression or from enhanced degradation of mistargeted proteins. Therefore, primary Nbea-KO effects on protein localizations or abundances in specific cell or synapse types may be much more pronounced. Moreover, the phenotypic manifestation of Nbea KO at different synapses may be influenced by different expression levels of the ubiquitous isoform, Lrba, or possibly even of other BEACH proteins. Given the high degree of sequence similarity of Nbea and Lrba (Wang *et al.* 2000), and the fact that they have a single orthologue in *C. elegans* and *Drosophila*, it seems likely that they are at least in part functionally redundant. No compensatory up-regulation of Lrba was detected in the Nbea KO mice (Fig. 1*B*), but the frequencies of expressed sequence tags indicate that the normal expression level of Lrba mRNA in whole mouse brain is already ∼25% of Nbea mRNA and might provide for partial compensation of Nbea deficiency, which might account for the marked but partial functional defects that we observe. Thus, our current results convincingly link Nbea to the structural and functional formation of central synapses, but more work will be needed to identify the molecular pathways and mechanisms involved.

The GTP-dependent and brefeldin-A-sensitive recruitment of Nbea mainly to endomembranes near *trans*-Golgi, reminiscent of the behaviour of Arf-GTPase-linked vesicle coat proteins (Wang *et al.* 2000), suggests a function relatively far upstream in a secretory pathway for membrane proteins. In spite of the prominent synaptic phenotype of Nbea deficiency, very little if any Nbea has been physically detected in presynaptic terminals by immunohistochemistry, and also its occurrence at postsynaptic plasma membranes is sparse (Wang *et al.* 2000), suggesting that Nbea re-dissociates from putative transport vesicles as they translocate towards the cell periphery. This upstream site of action makes it plausible that by the time the impact of Nbea ablation arrives at the cell periphery, it is pleiotropic

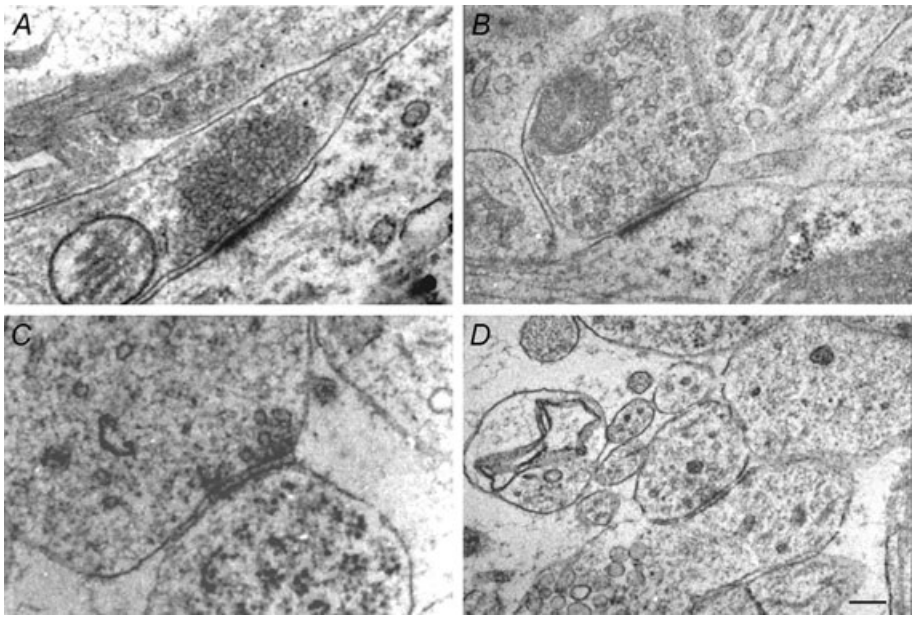

Figure 6. Ultrastructure of brainstem synapses in immersion-fixed, fetal wild-type and neurobeachin-deficient mice
A–D, electron micrographs of presumptive asymmetric (*A* and *B*) and symmetric (*C* and *D*) synaptic contacts in the rostral ventrolateral medulla (RVLM) of littermate WT (*A* and *C*) and KO animals (*B* and *D*) at embryonic day E18. Scale bar for *A–D*, 0.5 μm.

and complex, affecting several functional dimensions of synapses and the abundances of several proteins. As a large multidomain protein, Nbea probably interacts with many partners, and the likely partial compensation of Nbea deficiency by Lrba or other BEACH proteins will further diffuse the phenotype. Interestingly, one of the proteins whose abundance we find affected by Nbea, Mint1, is also implicated in Arf-dependent membrane protein traffic between the trans-Golgi network and the synapse (Shrivastava-Ranjan *et al.* 2008).

The pleiotropy of phenotypes that may be connected to a multi-domain protein such as Nbea makes it difficult to distinguish direct effects of the deletion from compensatory mechanisms that a mutant neuron may use to maintain its homeostasis, e.g. by using other membrane traffic mechanisms. However, given the multi-domain structure and far-upstream location of Nbea in the secretory pathway, even the complex phenotype described here in our study appears remarkably specific because many aspects of neuronal function that depend on exocytotic processes (cell numbers, viability, migration, membrane excitability, process growth, axon targeting, overall brain architecture, etc.) are largely unchanged in Nbea-deficient animals. In contrast, not just one but several synaptic proteins are reduced, synaptic morphology is compromised and synaptic function of both excitatory and inhibitory contacts is impaired, suggesting that Nbea indeed has a particular role in the formation and function of central synapses (this study), thereby extending an earlier observation that also aspects of peripheral synapses (NMJs) are affected by Nbea (Su *et al.* 2004).

At the NMJ of their Nbea KO mice, Su *et al.* (2004) determined a complete block of evoked transmission whereas nerve conduction, NMJ morphology and miniature quantal release were normal. This previous study and our current results consistently point to a crucial role of Nbea in synaptic function, in particular to stimulus–release coupling. However, there are also several important differences between the phenotypes of NMJs and central synapses.

(i) Nbea-deficient motoneurons form NMJs that exhibit normal AP-independent miniature neurotransmitter release (mepps) but are totally unable to sustain evoked AP-dependent responses (Su *et al.* 2004). In contrast, our analysis of central synapses showed that both AP-dependent (evoked or spontaneous) and AP-independent (miniature) synaptic transmissions are severely impaired. Such differential impacts on CNS synapses *versus* NMJs have also been observed in KO mice for other synaptic proteins: for example, in the Munc13-1/2-DKO mice evoked and miniature synaptic transmission is entirely abolished in the hippocampus (Varoqueaux *et al.* 2002) while both parameters are reduced but still present at NMJs (Varoqueaux *et al.* 2005). SNAP-25 mutant mice present increased miniature transmission at the NMJ (Washbourne *et al.* 2002), but almost abolished miniature transmission in cortical slices (Tafoya *et al.* 2006), with evoked neurotransmission completely impaired at both synapses. Together these results from our and previous studies suggest that physiologically relevant differences exist between the presynaptic release machineries of central and peripheral synapses.

(ii) We observed that the amplitudes of mIPSCs and sIPSCs are significantly reduced in Nbea-KO mice. At the NMJ in contrast, the function of postsynaptic AChRs is normal and the absence of evoked epps does not involve disruption of postsynaptic components (Su *et al.* 2004). Thus, our data point to an additional postsynaptic role of Nbea at least at inhibitory synapses, even though the related phenotype is less prominent than the putatively presynaptic changes. Aspects of postsynaptic signal propagation not addressed by our analyses may be responsible for the reduced sIPSC and mIPSC amplitudes (Fig. 3), even though the overall abundances of inhibitory neurotransmitter receptors were unaffected (Fig. 5). For example, immunoblot analysis does not discriminate between synaptic and extrasynaptic receptors, or between receptors on the plasma membrane and in endomembrane reservoirs, and will not necessarily detect perturbations of plasma membrane expression, postsynaptic integration or clustering of receptors unless these lead to enhanced receptor degradation. A postsynaptic role of Nbea would also be consistent with previous immuno-electron microscopy, which demonstrated localization of Nbea at tubulovesicular endomembranes within dendrites, and particularly at a minority of postsynaptic plasma membranes including, apparently, inhibitory synapses between mossy fibre terminals and Golgi cell dendrites of cerebellar glomeruli (Wang *et al.* 2000).

(iii) Despite the complete absence of evoked synaptic transmission, the number, structure and maturation of NMJs seemed normal (Su *et al.* 2004). Also in our own Nbea KO mice, the light-microscopic appearance of NMJs stained with fluorescent-labelled α-bungarotoxin in E18 diaphragm was normal (M.D., F. Varoqueaux & M.W.K., data not shown). In contrast, our EM results show a reduced density of type 1 synapses in the brainstem of Nbea-KO mice at E18, indicating that in the central nervous system the Nbea deficiency also manifests morphologically. As a note of caution, the reduced density of asymmetric contacts may reflect a delay of developmental maturation of excitatory synapses, balanced by a higher density of immature 'intermediate junctions' that may be morphologically classified as symmetric junctions and may obscure possible effects also on the density of actual type 2, inhibitory synapses. Reduced synapse density may contribute to the presynaptic phenotype described above, e.g. reduced

frequencies of mPSCs and sPSCs in central synapses of Nbea KO mice. In particular, the 70% reduction of the density of type 1 synapses is potentially sufficient to explain the 40% reduction of sEPSC frequency. However, it is unlikely that the 70% reduction of type 1, or the 50% reduction of total, synapse density alone can account for the 5.6- and 14-fold reductions of mEPSC and mIPSC frequencies, suggesting that genuine presynaptic functions such as vesicle fusion probability are also impaired in Nbea KO neurons.

Finally, the synaptic phenotype of Nbea-deficient mice is of medical interest because genetic studies have linked heterozygous Nbea gene rearrangements to cases of autism (Ritvo *et al.* 1988; Steele *et al.* 2001; Smith *et al.* 2002; Castermans *et al.* 2003; Savelyeva *et al.* 2006). Autism spectrum disorders are believed to be a disorder of early synaptic development (Zoghbi, 2003), and their aetiology may involve an 'excitatory–inhibitory imbalance' of synaptic activity (Persico & Bourgeron, 2006). By impairing inhibitory transmission more severely than excitatory transmission (Figs 2 and 3), Nbea haploinsufficiency may contribute to such an imbalance. Using similar experimental strategies as employed in this study, we also observed electrophysiological imbalances in analyses of neurexins and neuroligins, two families of synaptic transmembrane proteins linked to autism (Missler *et al.* 2003; Varoqueaux *et al.* 2006; Zhang *et al.* 2005), and of methyl-CpG-binding protein 2 (MeCP2), the molecule underlying the autistic spectrum disorder Rett syndrome (Medrihan *et al.* 2008). These and other studies suggest that mutations in genes as divergent as a transcriptional repressor or a cell adhesion protein may contribute to a common pathomechanism that manifests itself at the synapse (Zoghbi, 2003). Nbea may contribute to this 'autism pathway' by filling the gap between disturbances of transcriptional regulation and modified abundances of synaptic effector proteins, for example through trafficking subsets of proteins to the pre- and/or postsynaptic compartments.

References

Castermans D, Wilquet V, Parthoens E, Huysmans C, Steyaert J, Swinnen L, Fryns JP, Van de Ven W & Devriendt K (2003). The neurobeachin gene is disrupted by a translocation in a patient with idiopathic autism. *J Med Genet* **40**, 352–356.

De Lozanne A (2003). The role of BEACH proteins in *Dictyostelium*. *Traffic* **4**, 6–12.

De Souza N, Vallier LG, Fares H & Greenwald I (2007). SEL-2, the *C. elegans* neurobeachin/LRBA homolog, is a negative regulator of lin-2/Notch activity and affects endosomal traffic in polarized epithelial cells. *Development* **134**, 691–702.

Drummond GB (2009). Reporting ethical matters in *The Journal of Physiology*: standards and advice. *J Physiol* **587**, 713–719.

Faigle W, Raposo G, Tenza D, Pinet V, Vogt AB, Kropshofer H, Fischer A, de Saint-Basile G & Amigorena S (1998). Deficient peptide loading and MHC class II endosomal sorting in a human genetic immunodeficiency disease: the Chediak-Higashi syndrome. *J Cell Biol* **141**, 1121–1134.

Finley KD, Edeen PT, Cumming RC, Mardahl-Dumesnil MD, Taylor BJ, Rodriguez MH, Hwang CE, Benedetti M & McKeown M (2003). Blue cheese mutations define a novel, conserved gene involved in progressive neural degeneration. *J Neurosci* **23**, 1254–1264.

Horton AC & Ehlers MD (2003). Neuronal polarity and trafficking. *Neuron* **40**, 277–295.

Jogl G, Shen Y, Gebauer D, Li J, Wiegmann K, Kashkar H, Kronke M & Tong L (2002). Crystal structure of the BEACH domain reveals an unusual fold and extensive association with a novel PH domain. *EMBO J* **21**, 4785–4795.

Khodosh R, Augsburger A, Schwarz TL & Garrity PA (2006). Bchs, a BEACH domain protein, antagonizes Rab11 in synapse morphogenesis and other developmental events. *Development* **133**, 4655–4665.

Lim A & Kraut R (2009). The *Drosophila* BEACH family protein, Blue Cheese, links lysosomal axon transport with motor neuron degeneration. *J Neurosci* **29**, 951–963.

Medrihan L, Tantalaki E, Sargsyan V, Aramuni G, Missler M & Zhang W (2008). Early postnatal changes in GABA receptor-mediated synaptic transmission in the MeCP2 mouse model of Rett syndrome. *J Neurophysiol* **99**, 112–121.

Missler M, Zhang W, Rohlmann A, Kattenstroth G, Hammer RE, Gottmann K & Sudhof TC (2003). α-Neurexins couple Ca^{2+} channels to synaptic vesicle exocytosis. *Nature* **423**, 939–948.

Missler M, Wolff A, Merker H-J & Wolff JR (1993). Pre- and postnatal development of the primary visual cortex of the common marmoset. II. Formation, remodelling and elimination of synapses as overlapping processes. *J Comp Neurol* **333**, 53–67.

Persico AM & Bourgeron T (2006). Searching for ways out of the autism maze: genetic, epigenetic and environmental clues. *Trends Neurosci* **29**, 349–358.

Ritvo ER, Mason-Brothers A, Menkes JH & Sparkes RS (1988). Association of autism, retinoblastoma, and reduced esterase D activity. *Arch Gen Psychiatry* **45**, 600.

Savelyeva L, Sagulenko E, Schmitt JG & Schwab M (2006). The neurobeachin gene spans the common fragile site FRA13A. *Hum Genet* **118**, 551–558.

Shamloula HK, Mbogho MP, Pimentel AC, Chrzanowska-Lightowlers ZMA, Hyatt V, Okano H & Venkatesh TR (2002). Rugose (rg), a *Drosophila* A kinase anchor protein, is required for retinal pattern formation and interacts genetically with multiple signalling pathways. *Genetics* **161**, 693–710.

Shiflett SL, Vaughn MB, Huynh D, Kaplan J & McVey Ward D (2004). Bph1p, the *Saccharomyces cerevisiae* homologue of CHS1/Beige, functions in cell wall formation and protein sorting. *Traffic* **5**, 700–710.

Shrivastava-Ranjan P, Faundez V, Fang G, Rees, H, Lah JJ, Levey AI & Kahn RA (2008). Mint3/X11γ is an ADP-ribosylation factor-dependent adaptor that regulates the traffic of the Alzheimer's precursor protein from the trans-Golgi network. *Mol Biol Cell* **19**, 51–64.

Simonsen A, Birkeland HCB, Gillooly DJ, Mizushima N, Kuma A, Yoshimori T, Slagsvold T, Brech A & Stenmark H (2004). Alfy, a novel FYVE-domain-containing protein associated with protein granules and autophagic membranes. *J Cell Sci* **117**, 4239–4251.

Smith JC, Ellenberger HH, Ballanyi K, Richter DW & Feldman JL (1991). Pre-Botzinger complex: a brainstem region that may generate respiratory rhythm in mammals. *Science* **254**, 726–729.

Smith M, Woodroffe A, Smith R, Holguin S, Martinez J, Filipek PA, Modahl C, Moore B, Bocian ME, Mays L, Laulhere T, Flodman P & Spence MA (2002). Molecular genetic delineation of a deletion of chromosome 13q12–>q13 in a patient with autism and auditory processing deficits. *Cytogenet Genome Res* **98**, 233–239.

Steele MM, Al-Adeimi M, Siu VM & Fan YS (2001). Brief report: A case of autism with interstitial deletion of chromosome 13. *J Autism Dev Disord* **31**, 231–234.

Su Y, Balice-Gordon RJ, Hess DM, Landsman DS, Minarcik J, Golden J, Hurwitz I, Liebhaber SA & Cooke NE (2004). Neurobeachin is essential for neuromuscular synaptic transmission. *J Neurosci* **24**, 3627–3636.

Tafoya LC, Mameli M, Miyashita T, Guzowski JF, Valenzuela CF & Wilson MC (2006). Expression and function of SNAP-25 as a universal SNARE component in GABAergic neurons. *J Neurosci* **26**, 7826–7838.

Varoqueaux F, Sons MS, Plomp JJ & Brose N (2005). Aberrant morphology and residual transmitter release at the Munc13-deficient mouse neuromuscular synapse. *Mol Cell Biol* **25**, 5973–5984.

Varoqueaux F, Sigler A, Rhee JS, Brose N, Enk C, Reim K & Rosenmund C (2002). Total arrest of spontaneous and evoked synaptic transmission but normal synaptogenesis in the absence of Munc13-mediated vesicle priming. *Proc Natl Acad Sci U S A* **99**, 9037–9042.

Varoqueaux F, Aramuni G, Rawson RL, Mohrmann R, Missler M, Gottmann K, Zhang W, Sudhof TC & Brose N (2006). Neuroligins determine synapse maturation and function. *Neuron* **51**, 741–754.

Verhage M, Maia AS, Plomp JJ, Brussaard AB, Heeroma JH, Vermeer H, Toonen RF, Hammer RE, Van Den Berg TK, Missler M, Geuze HJ & Südhof TC (2000). Synaptic assembly of the brain in the absence of neurotransmitter secretion. *Science* **287**, 864–869.

Wang JW, Howson J, Haller E & Kerr WG (2001). Identification of a novel lipopolysaccharide-inducible gene with key features of both A kinase anchor proteins and chs1/beige proteins. *J Immunol* **166**, 4586–4595.

Wang JW, Gamsby JJ, Highfill SL, Mora LB, Bloom GC, Yeatman TJ, Pan TC, Ramne AL, Chodosh LA, Cress WD, Chen J & Kerr WG (2004). Deregulated expression of LRBA facilitates cancer cell growth. *Oncogene* **23**, 4089–4097.

Wang X, Herberg FW, Laue MM, Wüllner C, Hu B, Petrasch-Parwez E & Kilimann MW (2000). Neurobeachin: A protein kinase A-anchoring, beige/Chediak-higashi protein homolog implicated in neuronal membrane traffic. *J Neurosci* **20**, 8551–8565.

Washbourne P, Thompson PM, Carta M, Costa ET, Mathews JR, Lopez-Bendito G, Molnar Z, Becher MW, Valenzuela CF, Partridge LD & Wilson MC (2002). Genetic ablation of the t-SNARE SNAP-25 distinguishes mechanisms of neuroexocytosis. *Nat Neurosci* **5**, 19–26.

Zhai RG, Vardinon-Friedman H, Cases-Langhoff C, Becker B, Gundelfinger ED, Ziv NE & Garner CC (2001). Assembling the presynaptic active zone: a characterization of an active zone precursor vesicle. *Neuron* **29**, 131–143.

Zhang W, Rohlmann A, Sargsyan V, Aramuni G, Hammer RE, Sudhof TC & Missler M (2005). Extracellular domains of α-neurexins participate in regulating synaptic transmission by selectively affecting N- and P/Q-type Ca^{2+} channels. *J Neurosci* **25**, 4330–4342.

Zoghbi HY (2003). Postnatal neurodevelopmental disorders: meeting at the synapse? *Science* **302**, 826–830.

Author contributions

M.W.K., M.M. and W.Z. initiated and directed the study; L.M., A.R., R.F., J.A. and M.D. performed the research; L.M., W.Z., A.R. and M.M. analysed the data; W.Z., M.M. and M.W.K. wrote the manuscript. All authors approved the manuscript.

Acknowledgements

We thank S. Strömberg, K. Kerkhoff and C. Hühne for excellent technical help. This work was supported by grants from Uppsala University, Vetenskapsradet (Medical Section) and Deutsche Forschungsgemeinschaft (DFG) to M.W.K., the DFG through the Research Center for Molecular Physiology of the Brain (CMPB) to W.Z., and the DFG Sonderforschungsbereich 629 Münster (grant SFB 629-B11) to M.M. L.M. was a recipient of a Lichtenberg fellowship awarded by the International MSc/PhD Program *Neurosciences* (Göttingen).